

A quantitative approach to select PMTs for large detectors

L. J. Wen ^{a, *} M. He ^a, Y. F. Wang ^a, J. Cao ^a, S. L. Liu ^a, Y. K. Heng ^a,
Z. H. Qin ^a,

^aInstitute of High Energy Physics, Chinese Academy of Sciences, Beijing 100049, China

Abstract

Photomultiplier tubes (PMTs) are widely used in neutrino and other experiments for the detection of weak light. To date PMTs are the most sensitive single photon detector per unit area. In addition to the quantum efficiency for photon detection, there are a number of other specifications, such as rate and amplitude of after-pulses, dark noise rate, transit time spread, radioactive background of glass, peak-to-valley ratio, etc. All affect the photon detection and hence the physics goals. In addition, cost is another major factor for large experiments. It is important to know how to properly take into account all these parameters and choose the most appropriate PMTs. In this paper, we present an approach to quantify the impact of all parameters on the physics goals, including cost and risk. This method has been successfully used in the JUNO experiment. It can be applied to other experiments with large number of PMTs.

Key words: neutrino detector, PMT selection, 20-inch PMT

*E-mail: wenlj@ihep.ac.cn

1 Introduction

Since the first detection of neutrinos in 1956 [1], photomultiplier tubes (PMTs) have been widely used in various neutrino detectors, particularly the ones using liquid scintillator or water as target. For neutrino detectors with PMTs, their performance drives the accuracy and resolution of the energy, position or tracking, and time measurements, and that is a critical factor to physics potential. Typical PMT specifications include photon detection efficiency, rate and amplitude of after-pulses, dark noise rate, transit time spread, radioactivity of glass, peak-to-valley ratio, etc.

The quantum efficiency of the photocathode is the most important factor that determines the PMT's ability to detect photons. The photon detection efficiency (PDE) is defined as $\frac{1}{S_n} \int_{S_{pc}} \epsilon_{QE} \cdot \epsilon_{CE} dS$ in this paper. It represents the overall efficiency by averaging the product of the quantum efficiency (ϵ_{QE}) and collection efficiency (ϵ_{CE}) over different positions of the photocathode. It should be pointed out that the actual photocathode area (S_{pc}) is usually smaller than the nominal area (S_n) given by the diameter of the PMT, thus the fraction of effective photocathode area should be considered when comparing different PMTs. The thickness and composition of the photocathode vary over the cathode and cause quantum efficiency non-uniformity. The collection efficiency predominantly depends on the design of the focusing electrodes.

The transit time spread (TTS) affects the position resolution of a point-like particle or the tracking resolution of an energetic charged particle, particularly for large scale detectors. The TTS is mainly affected by the shape of the PMT's glass bulb, the design of the focusing electrodes and their location, as well as the operating voltage. For large area PMTs, simultaneous optimization of TTS and PDE was found to be difficult, particularly if requiring the top and the equator of PMT's glass bulb to have the same transit time. In some use case, the equator region can be masked to guarantee good TTS throughout the photocathode, resulting in less effective photocathode area.

Dark noise is mainly caused by the thermionic emission from the photocathode. PMTs with high quantum efficiency or a large photocathode intrinsically have larger probability of thermionic emission. Random coincidences of PMT dark noise will trigger the detector and create fake events, then the rate of dark noise affects the detector's energy threshold and hence affects low energy neutrino studies. The accidental coincidence of dark noise with physical signal degrades the energy resolution. Operating at low temperature helps to suppress the thermionic emission.

After-pulses are caused by the ion feedback from the ionization of the residual gas or the amplification process. The operating voltage affects the time distribution of after-pulses. Pre-pulses are caused by a photon directly striking the collection electrode without being reflected or absorbed by the glass or photocathode. Both after-pulses and pre-pulses affect the energy measurement.

The radioactivity of PMT's glass is an issue for low background experiments. The glass and the other components of the assembly inside the PMT should be screened before production till finding the clean ones that satisfy the low radioactivity budget.

Neutrino oscillation studies require high precision measurements. Future large detectors will be on the tens or hundreds of kton scale. Tens of thousands of PMTs will be needed if using liquid scintillator or water as target, and the impact of PMT parameters on physics goals is more sensitive comparing to a small scale detector. The PMT choices of some recent neutrino detectors are listed in Table. 1. The small and median scale detectors such as Daya Bay [2], Borexino [3], and SNO+ [4, 5] choose 8-inch PMTs, and some of them use light concentrators to enlarge the photon collection. The large scale detectors such as KamLAND [6, 7], Kamiokande-II [8], Super-K [9], JUNO [10, 11] and Hyper-K 1TankHD [12] unexceptionally use larger area PMTs. Most of the detectors in Table. 1 choose only one type of PMT. However, using a combination of different types of PMTs may enhance the physics potential if their performances are complementary. Note that R&D is still ongoing before the selection of the PMTs for Hyper-K will be finalized. Herein, the selection of JUNO PMTs is discussed.

Making the right choice of PMTs for large scale detectors is not an easy task. For different physics topics, each PMT characteristic affects the physics goals in a different way. The impact of all PMT parameters should be taken into account, and different types of PMTs need to be compared. Cost is certainly a critical factor. The risk regarding delivery capability and schedule also need to be considered. We need a quantitative approach to choose the most appropriate PMTs, considering the above factors and various physics goals.

The remaining part of this paper is organized as follows: In Sec. 2, we briefly introduce future large detectors using PMTs. Two types of large area PMTs, namely the MCP-PMTs and dynode-PMTs, are discussed in Sec. 3. In Sec. 4, we describe a quantitative approach to optimize the PMT choices for large neutrino detectors, which takes into account the physics performance, cost and risk, and the selection of JUNO PMTs is given as an example. Finally, we summarize our study and discuss its prospects in Sec. 5.

2 Future large detectors using PMTs

2.1 JUNO

The JUNO experiment [10, 11] is under design and construction, and its central detector is an excellent example of future large liquid scintillator detector. The primary goal of JUNO is to determine the neutrino mass ordering. In order to obtain an energy resolution better than $3\%/\sqrt{E(\text{MeV})}$, maximizing the photon collection has been the most critical factor driving the R&D programs and the detector design. The JUNO central detector consists of 20 kton purified liquid scintillator and two independent PMT systems. The large PMT

Table 1: PMT selection for some experiments.

Experiment	Target mass	PMT type	PMT number
Daya Bay	20 ton ^a	8-in. (R5912 ^b)	192
Borexino	300 ton	8-in. (EMI9351 ^c)	2,212 ^d
SNO+	780 ton	8-in. (R1408 ^b)	\sim 9,300 ^e
KamLAND	1 kton	20-in. (R3600 ^b)	1,325 ^f
		17-in. (R7250 ^b)	554 ^f
Kamiokande-II	3 kton	20-in. (R1449 ^b)	948
Super-K	50 kton	20-in. (R3600 ^b)	11,146
JUNO	20 kton	20-in. ^g	\sim 18,000
Hyper-K 1TankHD	260 kton	20-in. ^h	40,000

^a This is for one antineutrino detector module of the Daya Bay experiment. ^b Produced by Hamamatsu Photonics K. K. ^c Produced by Thorn EMI Electronics, which was merged by ET Enterprises Limited later. ^d About 1,800 were equipped with light concentrators, and the remaining PMTs without light concentrators were used for distinguishing muon tracks in the buffer and point-like events in the scintillator. ^e Each PMT was equipped with a 27 cm diameter concentrator. ^f 554 are older Kamiokande 20-in PMTs and 1,325 are a newly developed, faster version masked to 17-in. ^g It is a combination of MCP-PMT (GDG-6201) produced by North Night Vision Technology Co. Ltd. and dynode-PMT (R12860) produced by Hamamatsu. ^h The selection of Hyper-K 20-in PMTs is still under R&D stage, see Ref. [12], thus the exact PMT type is not decided yet.

system has approximately 18,000 20-inch PMTs providing \sim 75% photocathode coverage, and the average photon detection efficiency of PMTs is required to be $>$ 27% at 420 nm. The small PMT system has approximately 25,000 3-inch PMTs located in the gaps among the 20-inch PMTs, providing an additional 3% photocathode coverage and serving as an independent calorimeter to calibrate the energy nonlinearity. It also enhances the energy and track measurements for cosmic muons and neutrino interactions. The water Cherenkov detector of the JUNO veto system will be equipped with approximate 2,000 20-inch PMTs.

2.2 Hyper-K

Based on the experiences of Super-Kamiokande [9], the next generation water Cherenkov detector, Hyper-Kamiokande [12, 13, 14], is under design. The Hyper-Kamiokande (Hyper-K) experiment continues to use the water Cherenkov ring-imaging technique to detect neutrino interactions and search for nucleon decays. The Hyper-K experiment has planned two tanks and the total water mass will be 0.516 Mton. The baseline design for the first tank, namely HK-1TankHD, is one cylindrical vertical tank and the dimension of the water volume is 74 m in diameter and 60 m in height. The inner active volume of the tank, is a cylinder of 70.8 m in diameter and 54.8 m in height. Hyper-K intends to keep 40% photocathode coverage as SK-IV, thus its inner detector is instrumented by approximate 40,000 inward-facing 20-inch PMTs. The outer volume, equipped with approximate 6,700 8-inch PMTs facing outwardly, acts as a veto for cosmic muons and determines if a neutrino interaction occurring inside the

inner detector is fully contained.

2.3 Neutrino telescopes

The running neutrino telescopes in water and ice (like ANTARES [15], IceCube [16]) used the so-called optical module which houses a single 10-inch PMT in a pressurized transparent vessel. The recent KM3NeT [17] experiment has been developing the multi-PMT optical module concept, which replaces the single large area PMT with 31 3-inch PMTs. Such design has a better granularity with an accurate photon counting, and potentially fast timing for multi event reconstruction. It is more robust against the Earth’s magnetic field and the loss of one single PMT. In addition, thanks to the external pressurized vessel, the risk of chain implosion of PMTs is largely suppressed. Thus Hyper-K takes this concept as one of its photosensor alternatives, and has been developing multi-PMT module with similar dimension as KM3NeT but using UV transparent acrylic to make the pressure vessel.

3 Characteristics of large area PMTs

The 20-inch PMTs were motivated by the Kamiokande experiment and invented in the 1980s [18]. The quality was improved with a “Venetian-blind” type dynode (Hamamatsu R3600) used in the Super-Kamiokande detector [19]. A version masked to 17 inches with a “box-and-line” type dynode (Hamamatsu R7250) was developed for the KamLAND detector [6], and it provided faster timing for vertex reconstruction. The above three experiments have demonstrated that large area PMTs have the best performance-to-price ratio for large scale detectors. However, due to technical difficulties of fabricating 20-inch PMTs, very limited options were available and there was little space for optimization in the past.

Since JUNO and Hyper-K were proposed in late 2000s, the baseline choice of their photosensors has been using 20-inch PMTs. The available 20-inch PMT at that time was still the Hamamatsu R3600 model, with an average quantum efficiency of $\sim 22\%$ and collection efficiency of 70% at ~ 390 nm [19]. It satisfied the early minimum requirement of Hyper-K inner detector photosensors [14]. Nevertheless, the PDE of R3600 model is only about half of the required PDE for JUNO. Thus a completely novel design using a Micro-channel Plate (MCP) in place of a dynode to amplify photoelectrons was proposed [20, 21]. The original design of large area MCP-PMT had the transmission photocathode coated on the front hemisphere and the reflection photocathode coated on the rear hemisphere to form nearly 4π coverage to enhance the PDE. In 2015, the quantum efficiency of transmission photocathode reached 30% with improved transfer bialkali-photocathode technology [22], and the reflection photocathode on the rear hemisphere was abandoned, which improved the transit time spread and suppressed the dark noise. Furthermore, several improvements were made to reach almost 100% collection efficiency, by optimizing the diameter of micro-channel

plate, the size and inclined angle of the micro-channel, the open area ratio, and particularly using atomic layer deposition technology [23]. As an outcome of maximizing the collection efficiency, it has relative larger transit time spread than the Hamamatsu dynode PMT.

During the MCP-PMT development process, Hamamatsu improved its dynode 20-inch PMTs with higher quantum efficiency photocathode and better box-and-line dynode design [24], and the new type R12860-HQE became available. Given the recent developments on large area PMTs, in the most recent Hyper-K design report [12] the minimum requirement on PDE was increased to 26% around 400 nm. Another new type of 20-inch PMT, the so-called hybrid photodetector, was developed to obtain better timing and charge resolution. It uses an avalanche photodiode (APD) to replace the dynode for the amplification of photoelectrons. To guarantee the collection efficiency on the small area of the APD, ~ 8 kV high voltage need be applied between the APD and photocathode, thus its safe use in water over many years needs to be demonstrated.

By 2015, the 20-inch MCP-PMTs delivered by NNVT company (North Night Vision Technology Co. Ltd.) had comparable performance with respect to the 20-inch dynode-PMTs from Hamamatsu. Their typical specifications are summarized in Table. 2.

Table 2: The typical specifications of the 20-inch MCP-PMT and dynode-PMT in 2015. The typical values, as well as the lower or upper limits, are listed.

Characteristics	MCP-PMT	Dynode-PMT (R12860)
Detection Efficiency ^a [%]	27, >24	27, >24
Dark noise rate ^b [kHz]	20, <30	10, <50
Radioactivity of glass [ppb]	²³⁸ U : <50	²³⁸ U : <400
	²³² Th : <50	²³² Th : <400
	⁴⁰ K : <20	⁴⁰ K : <40
Transit Time Spread ^c (FWHM) [ns]	12, <15	2.7, <3.5
Pre-pulsing/After-pulsing [%]	<1 / <2	<1.5 / <15
Rise time/Fall time ^d [ns]	2 / 12	5 / 9
Peak-to-Valley ratio	3.5, >2.8	3, >2.5

^a The quoted detection efficiency refers to 420 nm photons. ^b Measured with a threshold of 1/4 p.e. ^c Measured on the top point of PMT. ^d The quoted rise and fall time refers to single photoelectron waveforms.

The 20-inch PMT's glass bulb is typically made by borosilicate glass, and it is non-trivial to control the radio-purity. The raw material components, such as silica sand, borax and boracic acid, aluminum hydroxide and industrial salt, should be screened until finding the clean ones that satisfy the low radioactivity budget. For the MCP-PMT's glass bulb, the projected radioactivity before mass production is listed in Table. 2, by summing up the selected materials according to their weight fractions. During the production cautious procedures were established and executed to control the radioactivity [25], and the final

radioactivity slightly differ from the original projection. Unfortunately it was impractical to follow the same approach to control the glass radioactivity for Hamamatsu products. Table. 2 also lists the projected radioactivity based on a few measured glass samples of Hamamatsu R12860.

The pre-pulsing ratio of MCP-PMTs is negligible because the surface of micro-channel plate has very low photoelectric conversion probability, whereas the dynode PMTs have a typical pre-pulsing peak about 10-90 ns before the main peak. The after-pulsing probability for MCP-PMTs is also lower, most likely due to the different structures between micro-channel plate and dynode and less residual gas which results in smaller ion feedback. As for other characteristics, both products guarantee good peak-to-valley ratio. The MCP-PMT has higher dark noise rate than the dynode PMT. The single photon electron waveforms of the MCP-PMTs have much faster rise time due to the fast amplification inside the micro-channels.

4 Optimize PMT selection for large detectors

For future large scale detectors, establishing a science-driven approach for the procurement of tens of thousands PMTs is highly desired. The selection should be based on the physics performance, price and risk. Below we propose a quantitative approach:

- Quantify the impact of each key parameter of PMT on physics goals;
- Convert the changes of physics performance into equivalent monetary cost, so that the impact on physics and real cost on purchasing PMTs can be normalized to the changes of overall project cost.
- Evaluate the risk, technology reliability, production schedule, service commitments, etc, and combine with the above outcome to make a decision.

Such approach is used in 2015 for the selection of JUNO 20-inch PMTs, and the diagram shown in Fig. 1 illustrates the concepts. The PMT selection is made by a selection committee based on three requirements: physics performance, cost, and risk factors. Different weights can be assigned to these different requirements and the physics performance is the most critical one. Taken JUNO as an example, the details of this approach are discussed below, particularly the merit of physics.

4.1 An example: JUNO 20-inch PMTs selection

4.1.1 How photo-sensors drive the sensitivity

In JUNO, the neutrino mass ordering is determined via precise spectral measurements of reactor antineutrino oscillations. Energy resolution is the most crucial factor to probe the

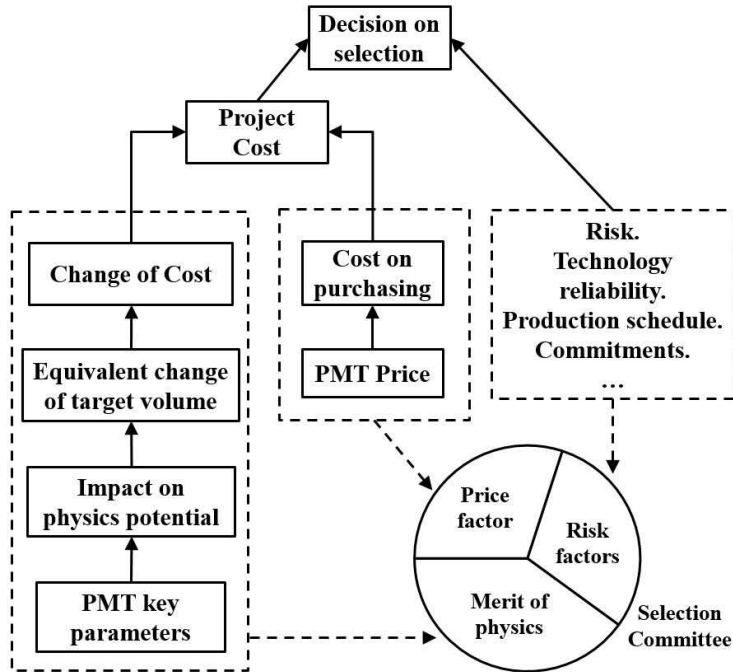


Figure 1: Diagram of the quantitative approach to select PMTs in JUNO.

interference effect of two fast oscillation modes. A conventional parametrization of energy resolution can be written as $\sigma_E/E = \sqrt{a^2/E + b^2 + c^2/E^2}$, where it consists of the stochastic term a , the constant term b and the noise term c . These three terms play different roles in affecting the sensitivity to neutrino mass ordering, thus an effective description is $\sqrt{(a^2 + (1.6b)^2 + (c/1.6)^2)/E}$ [10]. The impact of the main PMT characteristics on energy resolution is summarized below.

- The PDE drives the stochastic term a , which is the most critical parameter for determining the neutrino mass ordering. The minimum required PDE for the JUNO 20-inch PMTs is 27%.
- The dark noise contributes predominantly to the noise term c . Occasionally dark noise coincides with a physical event and degrades the energy resolution.
- The constant term b can be caused by the Cherenkov process, quenching effects, instability of detector response, residual energy errors after non-uniformity correction, and non-linearity of the electronics. For a large liquid scintillator detector like JUNO, the non-zero transit time spread degrades the vertex resolution [26] and consequently propagates into the energy error through non-uniformity correction, and eventually contributes to the constant term of the energy resolution.
- The pre-pulses arrive a short time prior to the main pulse, and they can directly overlap with true photons. After-pulses have instead a wider time distribution. Because the electron anti-neutrinos are detected via the inverse beta decay reaction, that consists

of a prompt positron signal and a delayed neutron-capture signal, the after-pulsing of the positron signal may fall into the signal window of the neutron signal and shift the neutron energy, or it could overlap with positron's own photons and shift the positron energy. Such effect will then hurt the accuracy of energy measurement and eventually degrade the sensitivity to neutrino mass ordering.

The total weight of the PMT glass in JUNO is ~ 140 tons, then the radioactivity of PMT's glass bulb would lead to non-zero background even with a water buffer between the liquid scintillator target and glass. A higher radioactivity requires tighter fiducial volume if keeping the same signal to background ratio, resulting in a degradation of sensitivity.

4.1.2 PMT performance merit

As discussed above, the variation of each PMT characteristic affects differently the sensitivity to neutrino mass ordering, by changing either the energy resolution or the background. In Fig. 2 (taken from Figure 13 in [10]), it shows the sensitivity ($\Delta\chi_{MH}^2$) contour as a function of the event statistics and the energy resolution. Thus, if setting a precondition of keeping the same projected sensitivity to neutrino mass ordering in six years, the change of energy resolution or background can be scaled to a corresponding change of the target mass. The increase or reduction in the total cost due to the change of the target mass, as well as the consequent cost change of acrylic sphere, number of PMTs, stainless steel structure and water pool excavation can be estimated according to their construction costs, and it quantifies the impact of the PMT performance.

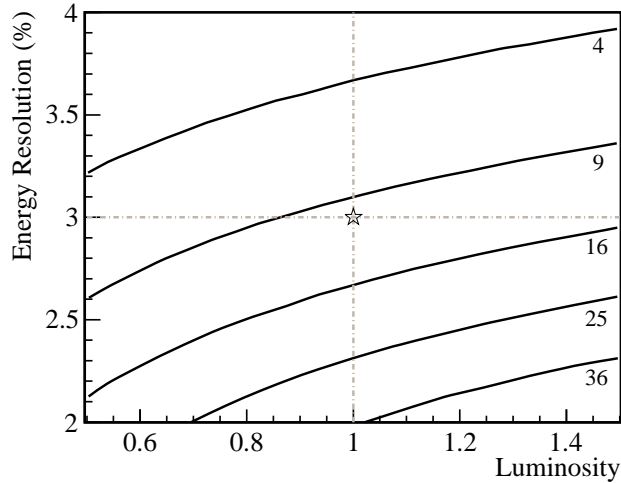


Figure 2: This plot is revised from Figure 13 in [10]. It shows the $\Delta\chi_{MH}^2$ contour as the function of the event statistics (luminosity) and the energy resolution, where the open star marker stands for the $3\%/\sqrt{E(\text{MeV})}$ energy resolution and the nominal running of six years with 20 kt target mass, 36 GW_{th} reactor power and 80% efficiency.

For parameters such as PDE, dark noise rate or transit time spread, any deviations

from the reference values were converted into changes of energy resolution by Monte Carlo studies. Their performance merit was further evaluated following the above method and parameterized in Eq. 1-3, where the reference values for detection efficiency (ϵ), dark noise rate (R_{DN}) and transit time spread (σ_{TTS}) are 27%, 20 kHz and 1 ns, respectively. Eq. 1-3 quantitatively describe how an improvement on PDE can be counteracted by an increase on dark noise rate or transit time spread. The right side of each formula is scaled to represent a unified price factor. For instance, if the PDE of all PMTs increases by 1%, the merit would be canceled if the price per PMT increases by ~ 1.2 k CNY, as indicated by Eq. 1 and Eq. 7 (see Sec. 4.1.3).

$$M_{DE} = (\epsilon - 27) \times 3.518 \quad (1)$$

$$M_{DN} = (20 - R_{DN}) \times 0.118 \quad (2)$$

$$M_{TTS} = -\log(\sigma_{TTS}) \quad (3)$$

Higher radioactivity of the PMT's glass would result in more accidental background in the fiducial volume. To keep the performance, we scale the liquid scintillator quantity to keep the same signal-to-background ratio in the fiducial volume. We convert the increment of liquid scintillator into a merit in Eq. 4, where R_U , R_{Th} and R_K refer to the ^{238}U , ^{232}Th and ^{40}K contaminations in the PMT glass, respectively. The measured values of low radioactive Schott glass, 22 ppb for ^{238}U , 20 ppb for ^{238}Th and 3.54 ppb for ^{40}K [27], were taken as the reference.

$$M_{Rad} = -\log \left[\frac{1}{3} \times \left(\frac{R_{Th}}{20} + \frac{R_U}{22} + \frac{R_K}{3.54} \right) \times 1.663 \right] \quad (4)$$

As for pre-pulses and after-pulses, a conservative assumption was made that, the pre-pulses and after-pulses which fall into the signal window would entirely contribute to the energy scale uncertainty. The measured time distributions of pre-pulses and after-pulses for each type of PMTs were used to calculate this effect. Furthermore, the dependence of the neutrino-mass-ordering sensitivity on the residual energy non-linearity is studied in Ref. [28]. Using those data, the merit for pre-pulses and after-pulses is parameterized as Eq. 5, where pp is the pre-pulse probability and ap is the after-pulse probability in percentage unit. The after-pulses have much less impact because of its wider time distribution.

$$M_{PA} = -0.693 \cdot (pp + 0.03 \cdot ap)^{1.56} \quad (5)$$

The merit of each PMT characteristic discussed above is shown in Fig. 3. The total merit of the PMT performance, denoted as M^{phys} , quantifies the overall impact of key parameters on physics goals:

$$M^{phys} = M_{DE} + M_{DN} + M_{TTS} + M_{Rad} + M_{PA} \quad (6)$$

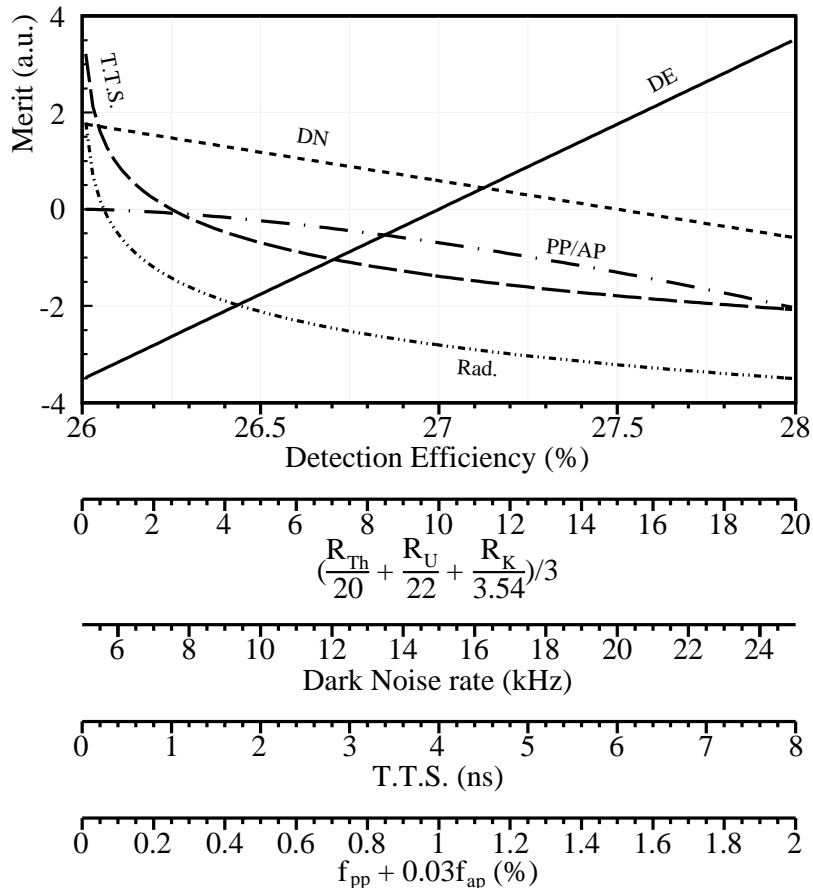


Figure 3: The PMT performance merit for physics as functions of different PMT characteristics, including the detection efficiency (M_{DE}), dark noise rate (M_{DN}), glass radioactivity (M_{Rad}), pre-pulsing and after-pulsing (M_{PA}), and transit time spread (M_{TTS}).

4.1.3 Selection strategy

Most experiments have only one vendor for one type of PMTs, as shown in Table. 1. However, one PMT type is more desirable in some characteristics but less satisfactory in other parameters. In addition, multiple vendors may reduce the risk if one of the vendors is not able to deliver. Thus, certain combination of different types of PMTs could be the best choice, but this causes complications to the selection strategy. The right selection strategy is extended from Fig. 1.

Multiple vendors participated in the bidding of JUNO's 20k PMTs. In order to evaluate possible combinations of different vendors with different award fractions, the total 20k PMTs were divided into twenty packages. Each vendor has the possibility to earn from 0 to 20 packages, and each vendor is required to provide quotation for each possibility. It is expected that the price per PMT is lower if the vendor earns more packages. In this case, if three vendors participate, 231 combinations should be considered, while if two vendors participate, only 11 combinations should be considered.

For each combination, we denotes that the i -th vendor earns N_i packages, and the corre-

sponding quotation of price per PMT is M_i , which is in 10k CNY unit. Then, we assign a price factor for the i -th vendor:

$$M_i^{price} = 30 \times (2.5 - M_i), \quad (7)$$

Furthermore, a safety factor $S_i = 1 - k_S \cdot \eta_i$ is assigned to the i -th vendor, where k_S is arbitrarily set to 0.15. The motivation is simple, the larger award fraction one vendor wins, the higher risk we takes. According to the PMT specifications that the i -th vendor guarantees, the merit of physics M_i^{phys} is given by Eq. 6. Finally, a selection committee gives overall justification to each vendor, denoted as $M_i^{committee}$ for the i -th vendor, with the main considerations on technology reliability, production schedule, and service commitments, etc. The highest and lowest marks among the individual committee members were removed and the average of the rest was taken as $M_i^{committee}$. In the end, the total merit of a specific combination is a summation over the vendors, as shown below:

$$S = \sum (M_i^{phys} + M_i^{price} + M_i^{committee}) \cdot S_i \cdot N_i / 20, \quad (8)$$

where the importance of M_i^{phys} , M_i^{price} and $M_i^{committee}$ are designed to be 40%, 30% and 30%, respectively. The final decision on PMT choice is the combination with the maximum total merit S .

4.1.4 Result

The public bidding for JUNO PMTs was opened in Dec, 2015 with two options: 20k 20-inch PMTs as the baseline, or 130k 8-inch PMTs as the alternative which has roughly equivalent total photocathode coverage. The bidders were required to provide the guaranteed PMT characteristics and the quotation for at least one of the two options. Three companies provided quotations for the 8-inch PMT option, but the total price was too high, thus this option was abandoned. Two of the three companies, NNVT and Hamamatsu, provided quotations with 20-inch MCP-PMT (GDG-6201) and dynode-PMT (R12860) products, respectively. Besides the main characteristics shown in Table. 2, other characteristics such as the mechanical strength under water, the long-term stability and the performance under Earth's magnetic field all satisfy the minimum specifications of JUNO. With the guaranteed PMT characteristics and quotations, the quantitative approach described in this section was used to compare different combinations of MCP-PMTs and dynode-PMTs. The combination of 15,000 20-inch MCP-PMTs and 5,000 20-inch dynode-PMTs gave the best total merit, thus it was the final choice of JUNO PMTs. Accordingly to the merit of physics performance (see Sec. 4.1.2), having a quarter of PMTs to be dynode type is mainly due to its good transit time spread which helps the vertex reconstruction.

5 Summary

Large area PMTs are likely the first choice of photon sensors for large liquid scintillator or water neutrino experiments which require high photocathode coverage. Besides photon detection efficiency, other characteristics such as dark noise rate, transit time spread, radioactive background of glasses, peak-to-valley ratio, etc, will affect the photon detection and hence affect the physics goals. It is theoretically and practically important to build a detector with maximum physics potential and minimum cost. This needs a science-driven approach to quantify the impact of all PMT parameters, including cost and risk, to the physics goals, and a selection strategy to make the decision. The quantitative approach described in this paper, which was successfully used for JUNO 20-inch PMTs selection, would set up a reference for future projects. After all, optimizing the selection of PMTs to build state-of-art neutrino observatories will enhance future scientific outputs.

ACKNOWLEDGMENTS

This work was supported by the Strategic Priority Research Program of the Chinese Academy of Sciences, Grant No. XDA10010100; the CAS Center for Excellence in Particle Physics (CCEPP) (for all authors).

References

- [1] Cowan C, *et al.* *Science* 124:103 (1956)
- [2] An FP, *et al.* *Nucl. Instrum. Meth.* A685:78 (2012)
- [3] G. Alimonti *et al.* [Borexino Collaboration], *Astropart. Phys.* **16**, 205 (2002) doi:10.1016/S0927-6505(01)00110-4 [hep-ex/0012030].
- [4] J. Boger *et al.* [SNO Collaboration], *Nucl. Instrum. Meth. A* **449**, 172 (2000) doi:10.1016/S0168-9002(99)01469-2 [nucl-ex/9910016].
- [5] S. Andringa *et al.* [SNO+ Collaboration], *Adv. High Energy Phys.* **2016**, 6194250 (2016) doi:10.1155/2016/6194250 [arXiv:1508.05759 [physics.ins-det]].
- [6] K. Eguchi *et al.* [KamLAND Collaboration], *Phys. Rev. Lett.* **90**, 021802 (2003) doi:10.1103/PhysRevLett.90.021802 [hep-ex/0212021].
- [7] S. Abe *et al.* [KamLAND Collaboration], *Phys. Rev. Lett.* **100**, 221803 (2008) doi:10.1103/PhysRevLett.100.221803 [arXiv:0801.4589 [hep-ex]].

- [8] K. Hirata *et al.* [Kamiokande-II Collaboration], Phys. Rev. Lett. **58**, 1490 (1987). doi:10.1103/PhysRevLett.58.1490
- [9] Y. Fukuda *et al.* [Super-Kamiokande Collaboration], Nucl. Instrum. Meth. A **501**, 418 (2003). doi:10.1016/S0168-9002(03)00425-X
- [10] An F, *et al.* [JUNO Collaboration] *J. Phys.* G43:030401 (2016)
- [11] Z. Djurcic *et al.* [JUNO Collaboration], arXiv:1508.07166 [physics.ins-det].
- [12] K. Abe *et al.* [Hyper-Kamiokande Collaboration], arXiv:1805.04163 [physics.ins-det].
- [13] K. Abe *et al.*, arXiv:1109.3262 [hep-ex].
- [14] [Hyper-Kamiokande Collaboration], KEK-PREPRINT-2016-21, ICRR-REPORT-701-2016-1.
- [15] M. Ageron *et al.* [ANTARES Collaboration], Nucl. Instrum. Meth. A **656**, 11 (2011) doi:10.1016/j.nima.2011.06.103 [arXiv:1104.1607 [astro-ph.IM]].
- [16] A. Achterberg *et al.* [IceCube Collaboration], Astropart. Phys. **26**, 155 (2006) doi:10.1016/j.astropartphys.2006.06.007 [astro-ph/0604450].
- [17] P. Bagley *et al.* [KM3NeT Collaboration], Technical Design Report for a Deep-Sea Research Infrastructure in the Mediterranean Sea Incorporating a Very Large Volume Neutrino Telescope,”
- [18] H. Kume, S. Sawaki, M. Ito, K. Arisaka, T. Kajita, A. Nishimura and A. Suzuki, Nucl. Instrum. Meth. **205**, 443 (1983). doi:10.1016/0167-5087(83)90007-8
- [19] A. Suzuki, M. Mori, K. Kaneyuki, T. Tanimori, J. Takeuchi, H. Kyushima and Y. Ohashi, Nucl. Instrum. Meth. A **329**, 299 (1993). doi:10.1016/0168-9002(93)90949-I
- [20] Wang Y. F. , et al. *Nucl. Instrum. Meth.* A695:113 (2012)
- [21] Wang Y. F. , “*Large Area MCP-PMT and its Application at JUNO*”, talk at *Neu-Tel2017*.
- [22] S. Qian, The 20 inch MCP-PMT R&D in China, Talk at the NNN 2016 workshop (2016)
- [23] https://en.wikipedia.org/wiki/Atomic_layer_deposition
- [24] S. Nakayama, Talk at the NNN 2014 workshop (2014)

- [25] X. Zhang, J. Zhao, S. Liu, S. Niu, X. Han, L. Wen, J. He and T. Hu, Nucl. Instrum. Meth. A **898**, 67 (2018) doi:10.1016/j.nima.2018.05.008 [arXiv:1710.09965 [physics.ins-det]].
- [26] Q. Liu, M. He, X. Ding, W. Li and H. Peng, JINST **13**, no. 09, T09005 (2018) doi:10.1088/1748-0221/13/09/T09005 [arXiv:1803.09394 [physics.ins-det]].
- [27] Robertson R. G. H., *SNO-STR-91-057*
- [28] Y. F. Li, J. Cao, Y. Wang and L. Zhan, Phys. Rev. D **88**, 013008 (2013) doi:10.1103/PhysRevD.88.013008 [arXiv:1303.6733 [hep-ex]].